Water Research 221 (2022) 118739

Contents lists available at ScienceDirect

Water Research

journal homepage: www.elsevier.com/locate/watres

Decolorization and control of bromate formation in membrane ozonation of humic-rich groundwater

Jakob Kämmler [a,b], Garyfalia A. Zoumpouli [c,d,e,1], Jörn Sellmann [a], Y.M. John Chew [d,e], Jannis Wenk [d,e,*], Mathias Ernst [a,b,*]

[a] Hamburg University of Technology, Institute for Water Resources and Water Supply, Am Schwarzenberg-Campus 3, 21073 Hamburg, Germany
[b] DVGW Research Centre TUHH, Am Schwarzenberg-Campus 3, 21073 Hamburg, Germany
[c] Centre for Doctoral Training, Centre for Sustainable Chemical Technologies, University of Bath, Bath BA27AY, United Kingdom
[d] Department of Chemical Engineering, University of Bath, Bath BA27AY, United Kingdom
[e] Water Innovation & Research Centre (WIRC), University of Bath, Bath BA27AY, United Kingdom

ARTICLE INFO

Keywords:
Ozone
Color
Membrane ozonation
Groundwater
NOM
Bromate

ABSTRACT

Membrane ozonation of bromide-containing, high-color natural organic matter (NOM) containing groundwater was performed using single-tube polydimethylsiloxane (PDMS) and multi-tube polytetrafluoroethylene (PTFE) membrane contactors, and compared to batch ozonation. For membrane ozonation, dissolved ozone concentration, water color (VIS_{436}), ultraviolet light absorption (UV_{254}) and bromate formation were correlated with ozone dose, ozone gas concentration, hydraulic retention time and Hatta number (Ha). NOM color removal of up to 45 % for the single-tube contactor and 17 % for the multi-tube contactor were achieved while containing bromate formation below 10 μg L^{-1}. Higher color removal using higher ozone doses was associated with high bromate formation i.e. >>10 μg L^{-1}. In membrane ozonation, low ozone gas concentrations, long hydraulic retention times and high Ha resulted in low dissolved ozone concentrations due to quenching of ozone by NOM. At specific ozone doses of < 0.5 mg O_3/mg DOC and Ha > 1, single-tube ozonation resulted in comparable results to batch ozonation while bromate formation was higher in the single-tube contactor at specific ozone doses > 0.5 mg O_3/mg DOC and Ha < 1. At comparable ozone doses and Ha, bromate formation in the multi-tube contactor was always higher compared to single-tube and batch ozonation. This could be associated with the uneven ozone distribution within the multi-tube contactor. Results show that ozone dose is the major driver for selectivity between bromate formation and NOM color removal in both membrane and batch ozonation. Bromate formation in membrane ozonation may be controlled by adjusting gas concentration, Ha and hydraulic retention time. Membrane module design and process parameters of membrane ozonation reactors significantly affect treatment performance and should be optimized for selective target compound removal over by-product formation.

Abbreviations: A, Absorbance; α, surface area of the membrane per unit volume of liquid (specific surface area); c, concentration; C_g, ozone concentration in the gas phase; $C_{L,out}$, ozone concentration in the effluent of the reactor; d, membrane inner diameter; δ, membrane thickness; $D_{g,O3}$, continuum gas diffusion coefficient; D_K, Knudsen diffusion coefficient; $d_{m,ln}$, logarithmic mean membrane diameter; $d_{m,o}$, membrane outer diameter; $D_{m,O3}$, diffusion coefficient of ozone in the membrane; D_{O3}, diffusion coefficient of ozone in water; DOC, dissolved organic carbon; $d_{s,h}$, hydraulic diameter of the shell; $d_{s,in}$, inner diameter of the shell; $d_{t,o}$, outer diameter of the central tube; ε, porosity; eq., equation; FL, humic fluorescence; Gz, Graetz number; H, Henry coefficient; Ha, Hatta number; L, membrane length; λ, wavelength; λ_r, reference wavelength; LC-OCD, liquid chromatography-organic carbon detection; k_G, gas-side ozone mass transfer coefficient; K_L, overall ozone mass transfer coefficient; k_L, liquid-side ozone mass transfer coefficient; k_m, ozone mass transfer coefficient within the membrane; k_{O3}, first-order ozone decay rate for the second (exponential) phase of reaction; IC, ion chromatography; M_{O3}, molecular weight of ozone; n, number of fibers; NOM, natural organic matter; ν, kinematic viscosity of water; O_3, ozone; OC, organic carbon; ·OH, hydroxyl radical; P, permeability of ozone through the membrane; PDMS, polydimethylsiloxane; PTFE, polytetrafluoroethylene; R, universal gas constant; Re, Reynolds number; r_p, membrane pore radius; S, spectral slope; Sc, Schmidt number; Sh_G, gas-side Sherwood number; Sh_L, liquid-side Sherwood number; SI, supporting information; S_m, solubility of ozone in the membrane material; $SUVA_{254}$, specific ultraviolet absorption at 254 nm (ratio of UV_{254} and DOC); T, absolute temperature; τ, membrane tortuosity; TOC, total organic carbon; u, water flow velocity; UV, ultra-violet (light); UV_{254}, ultra-violet light absorbance at 254 nm; VIS, visible (light); VIS_{436}, visible light absorbance at 436 nm; WHO, world health organization.

* Corresponding authors.
E-mail addresses: jhw46@bath.ac.uk (J. Wenk), mathias.ernst@tuhh.de (M. Ernst).
[1] Present address: Cranfield Water Science Institute, Cranfield University, College Road, Cranfield MK43 0AL, UK

https://doi.org/10.1016/j.watres.2022.118739
Received 3 February 2022; Received in revised form 29 May 2022; Accepted 10 June 2022
Available online 11 June 2022

1. Introduction

Ozonation is a versatile oxidation technology that is widely used in water treatment for disinfection, taste, color and odor control, and trace contaminant removal (Crittenden et al., 2012). The two major oxidants in ozonation are ozone (O_3) and the hydroxyl radical (·OH) formed during ozone decay (Gottschalk et al., 2010; von Sonntag and von Gunten, 2012). In the treatment of groundwater, ozonation is used for color removal (Lo Tan and Johnson, 2001; Rittmann et al., 2002), in conjunction with biofiltration for natural organic matter (NOM) removal to reduce disinfection by-product formation during subsequent chlorination (Tubić et al., 2011), and for disinfection (Tyrovola and Diamadopoulos, 2005). Similarly, ozonation has been applied in combination with groundwater recharge for disinfection, NOM and trace organic compound removal (Hübner et al., 2012; Zucker et al., 2015), and in direct and indirect potable water reuse (Gerrity and Snyder, 2011; Hooper et al., 2020). However, research on groundwater applications for ozone, including groundwater remediation is still limited (Ying et al., 2021).

NOM is a complex polymeric bulk material consisting of aromatic and non-aromatic moieties derived from the decomposition of terrestrial plants and algae (Brezonik and Arnold, 2011; Leenheer and Croué, 2003). Dissolved NOM occurs ubiquitously in natural waters at dissolved organic carbon (DOC) concentrations of up to more than 100 mg DOC L^{-1}, while mostly in the range of 0.5–10 mg DOC L^{-1} (Frimmel, 1998; Sillanpää, 2015). Presence of NOM affects water treatment processes and drinking water quality in many ways, for example as membrane foulant and during coagulation processes, as cause of taste, color and odor issues, as major scavenger of chemical oxidants, including ozone, and as precursor of disinfection-by-products (Alhweij et al., 2022; von Gunten, 2018). Consequently, understanding physical, biological and chemical interactions of NOM during water treatment is key to assess process performance and implications on final drinking water quality. Groundwater NOM concentrations are typically below 4 mg DOC L^{-1} (Regan et al., 2017; Rutlidge et al., 2021), with a global median of 1.2 mg DOC L^{-1} (McDonough et al., 2020). Comparatively high NOM concentrations of up to 10 mg DOC L^{-1} occur in some groundwaters in Northern Germany, which is specifically associated with undesired elevated water color when such groundwaters are used for drinking water production (Schulz, 2020).

NOM has high reaction rates with both ozone and hydroxyl radicals (von Sonntag and von Gunten, 2012). The reactivity of NOM with ozone can vary with its specific composition and the chemical structure of its compounds (Buffle et al., 2006; Westerhoff et al., 1999). Ozone itself reacts preferably by electrophilic addition with electron-rich moieties in NOM such as double-bonds and activated aromatic moieties such as phenols (Önnby et al., 2018) while hydroxyl radicals formed during ozonation react less specifically and can also oxidize less electron-rich moieties (Remucal et al., 2020). Ozonation induces reduction of spectroscopic, i.e., light-absorbing and light-emitting, properties of NOM, such as specific ultraviolet absorbance ($SUVA_{254}$) and fluorescence (Leresche et al., 2019), and its electron donating capacity (Rougé et al., 2020; Walpen et al., 2020). Specifically, ozone attacks the aromatic moieties of NOM, that define its optical properties (Sharpless and Blough, 2014), via electrophilic addition followed by ring cleavage (Wenk et al., 2013).

The presence of naturally occurring bromide (Br^-) in groundwater may complicate the ozonation process. During ozonation, Br^- reacts with ozone to form bromate (BrO_3^-) (Sobhani et al., 2012; von Gunten, 2003; von Sonntag and von Gunten, 2012). Bromate is a regulated by-product of ozonation, limited to maximum drinking water concentrations of 5 µg L^{-1} in the Netherlands (for disinfection) (Drinkwaterbesluit, 2011) or 10 µg L^{-1} in many other countries (EU, 1998; USEPA, 2009; WHO, 2017). Formation of bromate depends on several parameters including ozone dose, bromide concentration, pH and alkalinity (Yang et al., 2019). Bromate formation is reduced in the presence of NOM due to an overall reduction of ozone and hydroxyl radical exposure (Song et al., 1996; Westerhoff et al., 1998) and reaction of hypobromous acid (HOBr), an intermediate of the bromate formation pathway, with NOM (Heeb et al., 2014; von Sonntag and von Gunten, 2012). To control bromate formation during ozonation of drinking water and wastewater, addition of ammonia, ozonation at decreased pH and addition of hydrogen peroxide (H_2O_2) have been applied (Pinkernell and von Gunten, 2001; Soltermann et al., 2017). These methods increase treatment effort by additional dosing needs of chemicals and possibly subsequent removal or neutralization, given regulated requirements for finished drinking water (e.g., in Germany, 0.5 mg L^{-1} ammonia, pH > 6.5, $CaCO_3$ dissolution capacity < 5 mg L^{-1} $CaCO_3$, 0.1 mg L^{-1} H_2O_2) (Trinkwasserverordnung, 2001). Moreover, H_2O_2 addition was shown to slightly decrease ultraviolet light (UV_{254}) absorption reduction and humic substances removal in surface water treatment (Beniwal et al., 2018; Stylianou et al., 2018a) and may therefore also result in lower color removal than ozonation alone. Thus, bromate mitigation methods without additional chemical dosing are attractive for groundwater decolorization.

Membrane ozonation has been suggested as an alternative ozone gas-transfer method over conventional bubble-based methods used in water treatment due to potential advantages such as enhanced ozonation efficiency and better process control, as reviewed recently (Merle et al., 2017; Schmitt et al., 2020). The main feature of membrane ozonation is the spatial separation of gas and liquid by a membrane. This allows adjusting for specific ozone doses needed for target compound removal by different combinations of ozone gas concentration and hydraulic retention time, which has been investigated for membrane-based peroxone oxidation (ozonation with H_2O_2 dosing) (Merle et al., 2017; Stylianou et al., 2018b). It was observed that a combination of long hydraulic retention times and low ozone gas concentrations resulted in significantly lower bromate concentrations compared to short hydraulic retention times and high ozone gas concentrations. The effect was ascribed to low dissolved ozone concentration by ozone quenching of H_2O_2. Dissolved organic matter can quench ozone at rates that outcompete the reaction of H_2O_2 with ozone (Buffle et al., 2006; Pocostales et al., 2010). Thus, it is hypothesized that dissolved ozone concentrations and bromate formation in membrane ozonation may be controlled in the presence of NOM.

In gas-liquid transfer processes with chemical reaction, including membrane ozonation, the ratio of chemical reaction rate to mass transfer rate is a critical parameter as it comprises information about the concentration profiles of the reactants in the liquid-side and the degree of mass-transfer limitation of the system (Beltrán, 1995). This ratio can be quantified with the Hatta number Ha, which can be calculated for the case of first-order ozone decay by using Eq. (1) (Charpentier, 1981). Eq. (1) applies the film theory that assumes a stagnant liquid film between the membrane surface and the well-mixed bulk liquid and is frequently used in membrane ozonation models due to its simplicity (Berry et al., 2017; Phattaranawik et al., 2005).

$$Ha = \frac{\sqrt{D_{O_3}\, k_{O_3}}}{k_L} \tag{1}$$

D_{O3} is the diffusion coefficient of ozone in water, k_L is the liquid-side ozone mass transfer coefficient and k_{O3} is the first-order ozone decay rate for the second (exponential) phase of reaction which depends on the ozone dose (Nöthe et al., 2009). Reactions are located completely or mainly in the bulk liquid for very slow (Ha < 0.02) and slow kinetic regimes (0.02 < Ha < 0.3). In the intermediate or moderately fast regime (0.3 < Ha < 3), reactions take place both in the liquid film and in the bulk liquid resulting in prevalently low bulk liquid ozone concentrations. At fast kinetic regimes (Ha > 3) ozone is completely depleted in the liquid film, inhibiting ozonation reactions in the bulk liquid. To our knowledge there are no studies investigating the effects of Ha on bromate formation in membrane ozonation directly.

The aims of this study were (1) to investigate if bromate formation in the ozonation of a colored groundwater could be controlled by membrane ozonation and (2) to study the effects of the process parameters, namely ozone dose, gas concentration, hydraulic retention time and Ha on the competition between NOM degradation and bromate formation. A single-tube membrane ozonation contactor with a non-porous polydimethylsiloxane (PDMS) membrane was used to study fundamental effects of these process parameters on ozonation performance of natural groundwater. A larger multi-tube contactor with porous polytetrafluoroethylene (PTFE) membranes was used to assess whether these findings were similar irrespective of membrane material and build. As an external benchmark, conventional (batch) ozonation was compared to the results of membrane ozonation.

2. Materials and methods

2.1. Water sample

A batch of 60 L of treated groundwater was sampled at a drinking water treatment plant in Northern Germany in February 2020. The water had undergone treatment with aeration, calcium hydroxide flocculation and softening, two-stage sand filtration and subsequent carbon dioxide removal by degassing. Ozonation relevant properties of the water are shown in Table 1.

2.2. Chemicals

Oxygen for ozone production was of 99.5 % purity (BOC, Guildford, UK) for membrane ozonation and of 99.95 % purity (Westfalen, Münster, Germany) for batch experiments. Chemicals and analytical consumables were purchased from Sigma Aldrich or Fisher Scientific. Ultrapure water (resistivity > 18 MΩ cm^{-1}) and deionized water were produced with a Milli-Q (Merck, Darmstadt, Germany) water purification system for batch ozonation or an ELGA (Veolia, Paris, France) system for membrane ozonation.

2.3. Experimental procedure

Membrane ozonation experiments were conducted using two different setups, described below. Batch ozonation was performed via addition of an ozone stock solution. Experiments were performed in duplicate at 16 ± 1 °C. Mean values and standard deviations were calculated from these duplicates.

2.3.1. Single-tube membrane ozonation

The first membrane ozonation setup, referred to as single-tube contactor (Fig. 1.a), consisted of a single tubular non-porous PDMS membrane (Silastic® tubing, Cole-Parmer, UK) fixed at the central axis of a glass cylinder and is described in detail elsewhere (Zoumpouli et al., 2018). Membrane specifications are summarized in Table 2.

Table 1
Properties of the treated groundwater used as feed water for membrane ozonation. *Iron and manganese values were not measured in the sample used in this study but are measured by the water supplier in regular intervals with consistent results.

Property	Value
pH at 17 °C/-	8.0 ± 0.1
Total organic carbon (TOC)/mg C L^{-1}	5.7
Dissolved organic carbon (DOC)/mg C L^{-1}	5.6
Bromide/µg L^{-1}	82
Total Alkalinity/mmol L^{-1}	1.6
UV absorbance at 254 nm (UV_{254})/m^{-1}	15.3
Specific UV absorbance at 254 nm ($SUVA_{254}$)/L mg^{-1} m^{-1}	2.73
Color measured as visible absorbance at 436 nm (VIS_{436})/m^{-1}	0.48
Iron*/mg L^{-1}	0.1
Manganese*/mg L^{-1}	<0.005

For single-tube membrane ozonation experiments, the gas flow rate through the contactor was set to 100 mL min^{-1} (gas residence time of 30 s). A flow split was used that by-passed a portion of the inlet gas directly into the waste stream to simultaneously achieve low ozone concentrations and low gas flow rates entering the contactor. Experiments with different ozone concentrations in the feed gas were performed (25 to 197 g O_3 m^{-3}). Both feed gas and feed water were supplied in single-pass continuous mode. The water flow rate was measured gravimetrically and set to 1.2, 2.6, 5.0 or 9.7 mL min^{-1}, resulting in hydraulic retention times in the membrane reactor of 2 to 20 s (see Table S1). Formation of few small gas bubbles was observed inside the membrane tube at water flow rates of 1.2 and 2.6 mL min^{-1} due to fast oxygen/ozone transfer through the membrane. The system was left to equilibrate for at least 10 min before samples were taken from a sampling port at the single-tube contactor outlet. The minimum time required to achieve stable ozone transfer conditions had been determined in previous experiments (Zoumpouli et al., 2018). Samples for dissolved ozone measurements were quenched with indigo (see section 2.4 for details) while samples for light absorbance and bromate measurements were not quenched but carefully filled from bottom to top with no headspace and stored in the dark at room temperature for several hours, allowing for reactions to proceed until complete ozone depletion.

2.3.2. Multi-tube membrane ozonation

The second membrane ozonation module, referred to as multi-tube contactor (Fig. 1.b), was a custom-made hollow fiber unit at half the size of commercial modules and provided by Markel Corp (Plymouth Meeting PA, USA). The module consisted of a stainless-steel housing containing 490 porous PTFE membrane fibers. Further details are listed in Table 2. The module was installed vertically and operated in either co-current or counter-current flow with gas in the shell and liquid in the lumen. Gas was distributed within the module through a perforated tube located at the central axis of the module (Figure S1).

For multi-tube membrane ozonation experiments, an oxygen flow rate into the ozone generator of 1000 mL min^{-1} was used resulting in a gas residence time in the membrane module of less than 1 min. Experiments with different ozone concentrations in the feed gas were performed at 25 to 71 g O_3 m^{-3}. The water flow rate was measured volumetrically and set to 400, 680 or 920 mL min^{-1}, resulting in hydraulic retention times of 26 to 60 s (see Table S2). At 400 mL min^{-1}, the liquid-side pressure was increased by partially closing the needle valve to avoid formation of gas bubbles, while the pump provided sufficient pressure at higher flow rates (see Table S2). The system was left to equilibrate for at least 4 min, to provide more than four times the hydraulic retention time in the module, before samples were taken. The experiments were performed in counter-current flow for water and ozone gas. At the lowest liquid-side flow rate of 400 mL min^{-1}, an additional setup with co-current flow was implemented by inverting the gas flow direction. Samples were taken with the same procedure as described for single-tube membrane ozonation.

2.3.3. Batch ozonation

Batch ozonation experiments were performed in 100 mL DOC-free glass flasks containing 70 mL of water sample, with injection of an ozone stock solution. The applied specific ozone doses were 0.1, 0.2, 0.4, 0.6, 1.0 and 1.5 mg O_3/mg DOC. Ozone for the batch experiments was produced from oxygen using a lab ozonizer (301.7, Sander, Uetze-Elze, Germany). Water for the stock solution was of ultrapure grade and maintained at the sample temperature of 16 °C during preparation. Ozone concentration in the stock solution was 21 ± 1 mg L^{-1} as measured by UV absorption (molar attenuation coefficient 3200 M^{-1} cm^{-1} at 260 nm) (von Sonntag and von Gunten, 2012). The injection of ozone stock solution was done using a syringe extended with PTFE tubing to ensure submerged ozone dosing. Samples were stirred with a PTFE-coated magnetic stirrer during ozone addition and for at least 20 s

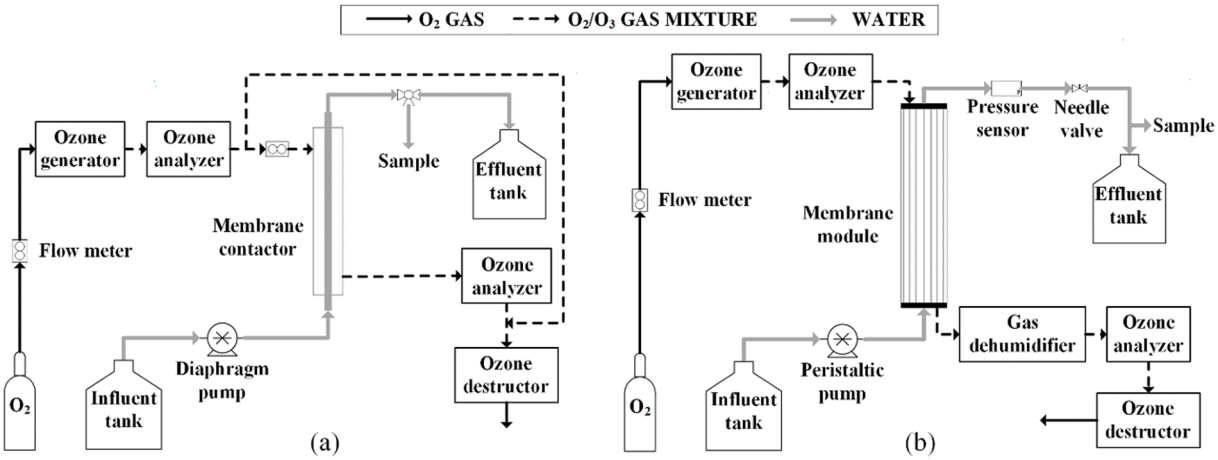

Fig. 1. a. Single-tube contactor and b. multi-tube contactor ozonation setups. Instrumentation details are listed in the SI, section S1.1.

Table 2
Specifications of the single-tube contactor and the multi-tube contactor. *Based on the inner diameter. **Maximum pore size provided by the manufacturer.

Membrane contactor	Single-tube contactor	Multi-tube contactor
Membrane outer diameter/mm	3.2	1.9
Membrane inner diameter/mm	1.6	1.5
Membrane length/cm	20	46
Number of membrane tubes	1	490
Lumen volume /mL	0.4	400
Shell volume, minus the lumen/mL	50	1000
Membrane surface area*/m^2	0.001	1.1
Membrane specific surface area*/m^2 m^{-3}	2500	2670
Membrane material	non-porous PDMS	porous PTFE
Membrane maximum pore size**/μm	-	0.82

afterwards for complete mixing. Samples were stored at 16 °C in the dark. Analysis took place on the subsequent day after filling up all water samples with ultrapure water to a volume of 100 mL. The resulting dilution factor of the water, 1.43, was multiplied with the analytical values for UV_{254}, VIS_{436} and bromate to allow comparison with the membrane ozonation results.

Kinetic batch experiments were performed for specific ozone doses of 0.5, 1.0 and 1.5 mg O_3 /mg DOC in a batch setup with a dispenser mounted on the flask from which samples were taken at regular time intervals. Ozone stock solution was added with a syringe via a side-socket equipped with a septum and cannula. Stock solution addition took place below the reactor water level for about 20 s before sampling at regular defined time intervals commenced. A lab dispenser was used for sampling for residual ozone measurements with indigo (see section 2.4 for details). Stirring was discontinued 60 s after stock solution addition to prevent volatilization of ozone. No significant loss of ozone in the reactor was found over the experimental duration of 20 min in tests using 20 mM H_3PO_4 at pH 2.

2.4. Analytical techniques

The concentration of dissolved (residual) ozone in the water outlet of each membrane contactor and in stock solution experiments was measured with the indigo method (Bader and Hoigné, 1981). All samples except for those for dissolved ozone, TOC and pH were filtered prior to analysis using 0.45 μm polypropylene syringe filters (VWR International, Radnor, US). Absorbance measurements at 254 and 436 nm and wavelength scans (190–700 nm, 0.5 nm increment) were performed with a Hach Lange DR 5000 spectrophotometer (Hach, Loveland, USA) using 5 cm quartz glass cuvettes. All absorbance measurements were corrected by the absorbance of ultrapure water. Bromate concentrations were measured by ion chromatography (IC) with post-column reaction and UV detection of triiodide (ISO, 2011). A Metrohm IC with an ASupp16 column (Metrohm AG, Herisau, Switzerland) was used. Bromide was measured by ion chromatography with UV detection using the same Metrohm IC with an ASupp5 column. TOC and DOC were quantified as non-purgeable organic carbon with the TOC analyser TOC-L (Shimadzu Corp., Kyoto, Japan) using combustion catalytic oxidation at 680 °C coupled with a nondispersive infrared sensor. The pH of the feed water was measured with a FE20 pH meter (Mettler Toledo, Leicester, UK).

2.5. Ozone mass transfer calculations

Although small ozone concentration differences between inlet and outlet gas were detected for both membrane ozonation contactors, it was not possible to accurately determine the transferred ozone dose from a gas-side mass balance. Therefore, UV_{254} reduction was used as a proxy for the ozone dose. This approach was chosen because UV_{254} has been established as a surrogate parameter for oxidant exposure in ozonation processes, e.g. for micropollutant degradation and bromate formation (Chon et al., 2015) or to quantify the formation of biodegradable organic carbon during ozonation (Li et al., 2017). Specific ozone doses applied in membrane ozonation were approximated from the results of the batch experiments, of which the ozone dose was known. For calculations see SI, section S1.3.

Ozone decay in natural waters is usually modeled as a biphasic process consisting of an initial rapid ozone consumption phase and a slower secondary phase, assuming first-order exponential ozone decay (Elovitz et al., 2000; Westerhoff et al., 1999). This secondary phase can be modeled using a first-order ozone decay rate k_{O3}, which was also used here to calculate Ha of membrane ozonation (Eq. (1)). To obtain k_{O3} of membrane ozonation experiments, an exponential fitting of k_{O3} (after 15 s of reaction) versus the ozone dose from kinetic batch experiments was used. The fitting was calculated from the data of ozone doses of 0.5, 1.0 and 1.5 mg O_3/mg DOC (Table S7, Figure S2). The fitting was performed in Origin (Originlab, Northampton, USA) with an exponential function of the form $y = y0 + A \bullet \exp(R_0 x)$, where y is the ozone decay rate k_{O3} in s^{-1} and x is the ozone dose in mg O_3/mg DOC (Figure S3). Fitting parameters are the offset y_0, the initial value A and the rate R_0. The results of the fitting were $y_0 = 0.0024\ s^{-1}$, $A = 0.30\ s^{-1}$ and $R_0 =$ -3.8 mg DOC/mg O_3. Using that function, the first-order ozone decay rate k_{O3} was estimated for each membrane ozonation experiment. Ha was calculated by using overall ozone decay rates k_{O3} determined at the contactor outlets accounting for the overall ozone dose that the water received.

The liquid-side ozone mass transfer coefficient k_L (Phattaranawik et al., 2005) was calculated by Eq. 2 from the liquid-side Sherwood number Sh_L, the diffusion coefficient of ozone in water at 16 °C, D_{O3}, and the membrane inner diameter $d_{m,in}$. The Sherwood number was calculated based on the Lévêque correlation (Lévêque, 1928) and is explained in detail in the SI, section S1.4. The gas-side and membrane mass transfer coefficients were calculated and presented in the SI, section S1.4, Table S5.

$$k_L = \frac{Sh_L \, D_{O_3}}{d_{m,in}} \tag{2}$$

3. Results and discussion

3.1. Ozone mass transfer in membrane ozonation

The two membrane contactors used in this study obtained different membrane materials and module geometry (Table 2). However, the experimental overall mass transfer coefficient was similar in both contactors (Table S5). The theoretical overall mass transfer coefficient in the multi-tube contactor was higher than the experimental one, which may be due to non-ideal flow conditions within the module. The experimental conditions for groundwater ozonation, i.e., feed-gas ozone concentrations and hydraulic retention times, were chosen to achieve a similar range of residual dissolved ozone concentrations for both membrane contactors. The range of residual dissolved ozone concentration at the contactor outlet was 0.0–6.4 mg L^{-1} for the single-tube contactor (Fig. 2.a) and 0.0–7.2 mg L^{-1} for the multi-tube contactor (Fig. 2.b). At the same dissolved ozone concentration, the transferred ozone dose may be higher in the multi-tube contactor due to increased hydraulic retention time and therefore increased ozone consumption within the module. Changing the flow mode to co-current in the multi-tube contactor decreased dissolved ozone concentrations slightly (Fig. 2. b), which was expected due to the decreasing concentration difference between gas and liquid side which is the driving force for mass transfer (Atchariyawut et al., 2007). Zero-outlet concentrations of ozone were measured at ozone doses below 2 mg L^{-1} in both contactors (Figure S4), indicating rapid initial ozone consumption. This is due to fast reactions of NOM and other water matrix constituents and is referred to as the immediate ozone demand (Schmitt et al., 2020). At ozone doses above the immediate ozone demand, which applies for hydraulic retention times of 9.2 and 20 s in the single-tube contactor and for all hydraulic retention times in the multi-tube contactor, dissolved ozone concentrations increased with both hydraulic retention time and ozone gas concentration, in agreement with previous studies (Kaprara et al., 2020; Stylianou et al., 2016; Zoumpouli et al., 2018). In fact, a linear relationship between dissolved ozone in groundwater and ozone gas concentration was observed when exceeding the immediate ozone demand (Fig. 2, Figure S4). Additional experiments with ultrapure water (i.e., without an ozone sink) with the multi-tube contactor (see Figure S5) resulted in similar slopes as for the ozonation of groundwater (e.g., for 60 s hydraulic retention time, m = 0.12 ± 0.003 for groundwater and m = 0.13 ± 0.003 for ultrapure water). However, a concentration offset in groundwater ozonation was visible due to the immediate ozone demand and resulted in negative y-intercepts (-2.0 ± 0.10 mg $L^{-1} \leq x_0 \leq$ -1.1 ± 0.13 mg L^{-1} in groundwater versus -0.90 ± 0.38 mg $L^{-1} \leq x_0 \leq$ 0.32 ± 0.45 mg L^{-1} in ultrapure water).

Liquid-side mass transfer coefficients k_L for the membrane contactors were calculated based on Eq. (2). The single-tube contactor exhibited generally higher k_L values than the multi-tube contactor (6.90 • 10^{-6} m $s^{-1} \leq k_L \leq$ 1.38 • 10^{-5} m s^{-1} for the single-tube contactor (Table S1) versus 4.87 • 10^{-6} m $s^{-1} \leq k_L \leq$ 6.43 • 10^{-6} m s^{-1} for the multi-tube contactor (Table S2).

Reaction conditions in the membrane ozonation contactors were compared based on the dimensionless Hatta number, Ha (Fig. 3). Ha values of 0.31–1.72 in the moderately fast regime (0.3 < Ha < 3) were obtained, indicating that reactions took place both in the liquid film and in the bulk. This is comparable to the membrane ozonation of NOM isolates at pH 7 and 2.66 ± 0.4 mg DOC L^{-1}, that resulted in Ha of 0.52–0.82 (Leiknes et al., 2005). Zero-outlet concentrations of dissolved ozone, which were obtained by a combination of short hydraulic retention times and low feed-gas ozone concentrations, were correlated with Ha > 1 in the single-tube contactor, indicating the liquid film as the main reaction zone (Leiknes et al., 2005). In multi-tube ozonation, a zero-outlet ozone concentration was obtained at Ha = 1.67 only. Dissolved ozone concentrations of the multi-tube contactor were slightly higher than in the single-tube contactor at similar Ha values. According to Eq. (1), similar Ha values imply lower k_{O3} and therefore higher ozone dose in the multi-tube contactor than in the single-tube contactor to make up for the lower k_L of the multi-tube contactor. Moreover, in the

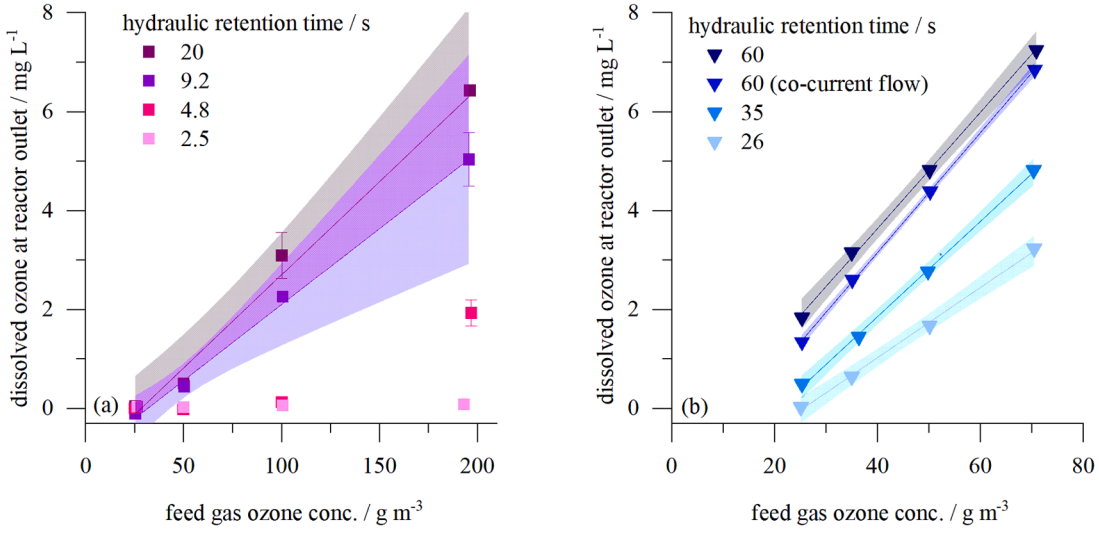

Fig. 2. Dissolved ozone concentration at the reactor outlet in membrane ozonation of groundwater (16 °C, pH 8.0, DOC 5.6 mg L^{-1}) with linear fits and 95% confidence intervals for a. the single-tube contactor (specific ozone dose 0.01–1.58 mg O_3/mg DOC); 20 s: x_0 = -1.1 ± 0.22 mg L^{-1}, m = 0.038 ± 0.003, R^2 = 0.99; 9.2 s: x_0 = -0.97 ± 0.17 mg L^{-1}, m = 0.031 ± 0.003, R^2 = 0.98; b. the multi-tube contactor (specific ozone dose 0.38–1.57 mg O_3/mg DOC); linear fit: 60 s: x_0 = -1.1 ± 0.13 mg L^{-1}, m = 0.12 ± 0.003, R^2 = 1.00; 60 s co-current: x_0 = -1.7 ± 0.05 mg L^{-1}, m = 0.12 ± 0.001, R^2 = 1.0; 35 s: x_0 = -2.0 ± 0.10 mg L^{-1}, m = 0.096 ± 0.002, R^2 = 1.0; 26 s: x_0 = -1.8 ± 0.11 mg L^{-1}, m = 0.071 ± 0.002, R^2 = 1.0; errors (±) given as standard errors.

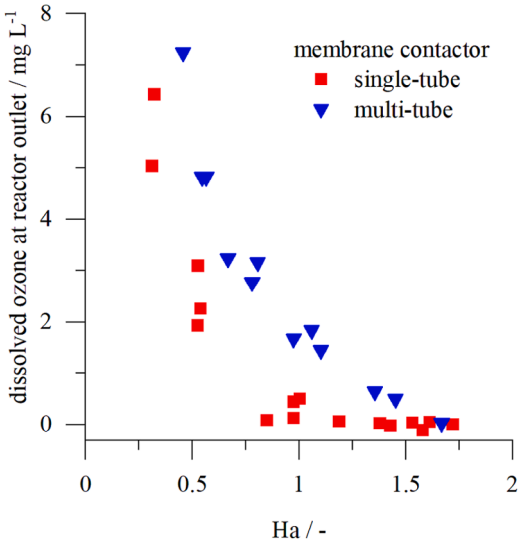

Fig. 3. Correlation of dissolved ozone concentration at the reactor outlet and Hatta number in membrane ozonation. Experimental conditions: 16 °C, pH 8.0, DOC 5.6 mg L^{-1}; specific ozone dose 0.01–1.58 mg O_3/mg DOC (single-tube contactor), 0.38–1.57 mg O_3/mg DOC (multi-tube contactor).

multi-tube contactor, a transversal ozone concentration gradient on the gas-side is established due to the distribution of ozone from a single central tube (see Figure S1 and Methods, section 2.3 for details). This implies that membrane fibers near the center receive more ozone than those located further towards the outer wall of the contactor. Inner fibers might have received higher specific ozone doses, resulting in depletion of fast-reacting NOM moieties and elevated overall residual ozone concentrations at the contactor outlet.

3.2. Transformation of groundwater NOM in batch ozonation

UV/VIS-absorbance spectra for groundwater as absolute values are shown for batch experiments in Fig. 4.a and the inlet Fig. 4.b covering the visible light region that showed low absorbance. NOM typically exhibits an exponential decrease in absorption with increasing wavelength that can be modeled with the function $A(\lambda) = A(\lambda_r) \bullet \exp(-S(\lambda - \lambda_r))$, where A is the absorbance at wavelength λ, λ_r is the reference wavelength, and S is the spectral slope (Twardowski et al., 2004). Fig. 4.c shows relative absorbance compared to the initial non-ozonated sample. Absorbance generally decreased steadily with increasing ozone dose and to similar extent for wavelengths below 350 nm (Fig. 4.c). At wavelengths above 350 nm a smaller decrease or even small increases in absorbance for wavelengths above 375 nm were observed at lower ozone doses. Color, i.e., absorbance at 436 nm was therefore increased at ozone doses below 0.4 mg O_3/mg DOC. Moreover, at these ozone doses, spectral slopes decreased (Figure S6). This is in contrast with previous findings of consistently increasing spectral slopes for NOM isolates with increasing ozone doses, including at low ozone doses (Wenk et al., 2013). To further investigate this phenomenon, liquid chromatography with subsequent organic carbon detection (LC-OCD) analyses and additional ozonation experiments with pre-filtered samples were conducted. LC-OCD chromatograms, data from the additional experiments and a detailed explanation are given in the SI, section S2.2, Figures S7 and S8. In short, the humic substances organic carbon (OC) peak shifted to smaller retention times at low ozone doses, indicating that high-molecular NOM with contribution to VIS_{436} was released from colloidal NOM fractions at ozonation. Pre-microfiltration (0.1 or 0.45 μm) of the samples reduced the increase in VIS_{436} at low ozone doses, which demonstrates that the NOM compounds with contribution to VIS_{436} originate from such colloidal NOM fractions.

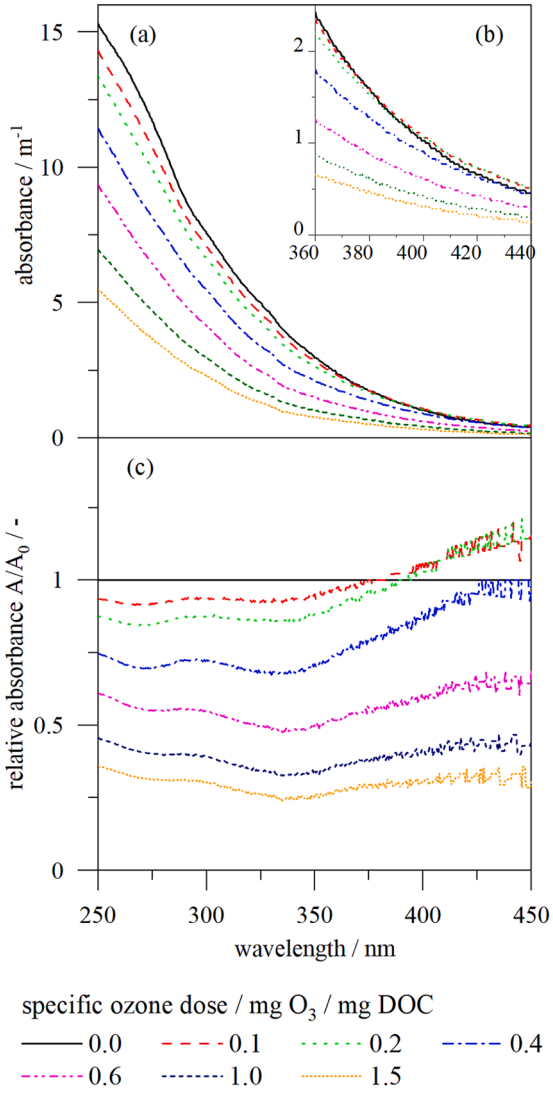

Fig. 4. a. UV/VIS-absorbance spectra of water samples for varying specific ozone doses of batch ozonation experiments (dilution by ozone stock solution considered by multiplication with the dilution factor of 1.43) b. inlet showing absorbance in m^{-1} for wavelengths from 360 to 440 nm c. Relative absorbance spectra regarding non-ozonated sample (0.0 mg O_3/mg DOC). Experimental conditions: 16 °C, pH 8.0, DOC 5.6 mg L^{-1}

3.3. Color removal and bromate formation in membrane and batch ozonation

Despite the initial visible absorbance increase at low ozone doses, which was similar across the three experimental setups, both membrane and batch ozonation led to a significant decrease in VIS_{436} from initially ≈ 0.5 m^{-1} to values under 0.2 m^{-1} at 1.5 mg O_3/mg DOC, the highest ozone dose tested (Fig. 5.a). VIS_{436} decrease at 1.0 mg O_3/mg DOC was ≈ 60 %, which was slightly lower than expected from previous studies on color removal in wastewater (color measured at 455 nm) (Wert et al., 2009) and groundwater (color measured at 408 nm) (Rittmann et al., 2002), both of which reported a color decrease of ≈ 80 % at 1.0 mg O_3/mg DOC. We attribute the lower decolorization efficacy in this groundwater sample to the initial increase of color at lower ozone doses (see section 3.2). Small variation in VIS_{436} at comparable ozone dose, i.e. at comparable UV_{254} reduction, was observed in the different ozonation setups. It is viable that the different ozone dosing mechanisms affected reaction conditions in the membrane contactors. If a significant amount of ozone reacts within the liquid film, i.e., at Ha > 1 (Leiknes

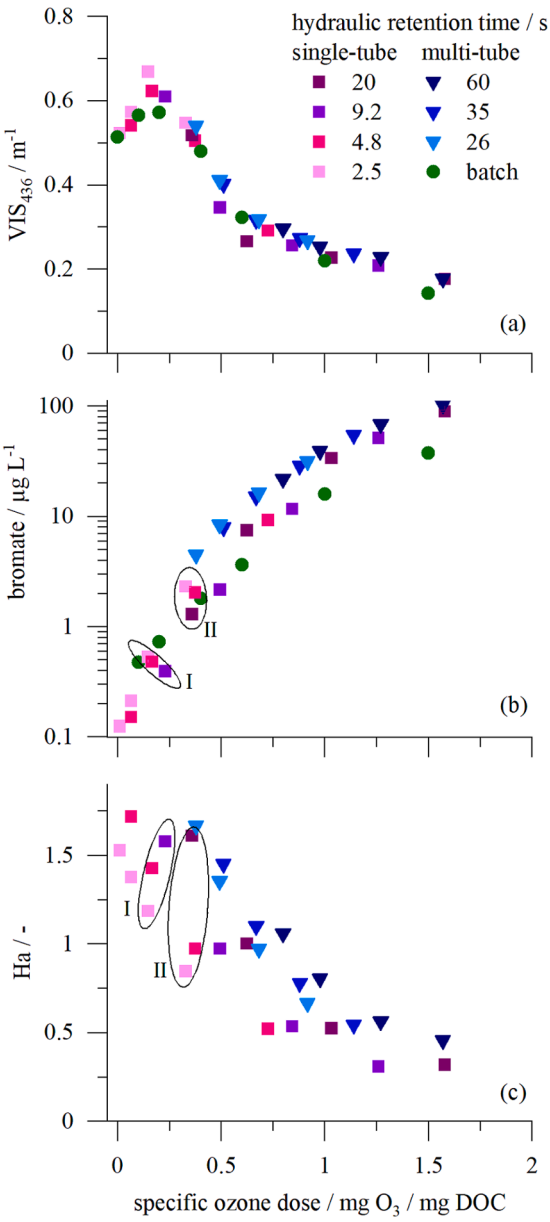

Fig. 5. a. NOM Color (VIS_{436}), b. bromate and c. Hatta number (Ha) as functions of specific ozone dose for batch (bullets), single-tube (squares) and multi-tube ozonation (triangles). Clusters I and II highlight data points of single-tube ozonation with comparable ozone doses and different bromate concentrations and Ha values in single-tube ozonation. Experimental conditions: 16 °C, pH 8.0, DOC 5.6 mg L^{-1}

et al., 2005), ozone and hydroxyl radical exposure of water constituents may vary spatially. In the liquid film, ozone may be consumed quickly by fast-reacting NOM moieties (Jansen et al., 2005). The hydroxyl radical exposure may not be affected by this, as it depends on the consumed amount of ozone and not the ozone exposure (Kwon et al., 2017). However, as Ha was in the moderately fast regime ($0.3 < Ha < 3$) for membrane ozonation experiments in this study, we believe that the effect of varied hydroxyl radical to ozone exposure ratios on UV_{254} and VIS_{436} was minor and within the experimental error. Results for color removal for the single-tube contactor were more scattered compared to the multi-tube contactor and batch ozonation. This is probably due to the larger variation of mass transfer conditions in the single-tube contactor (ratio of highest and lowest k_L = 2.0, ratio of highest and lowest ozone feed gas concentration = 8.0, Table S1) compared to the multi-tube contactor (ratio of highest and lowest k_L = 1.3, ratio of highest and lowest ozone feed gas concentration = 2.8, Table S2), which may have expanded the range of results and underlines an association between mass transfer conditions and final water quality.

Bromate concentrations remained generally below the WHO guideline value of 10 µg L^{-1} for ozone doses below 0.5 mg O_3/mg DOC for all ozonation setups (Fig. 5.b). At higher ozone doses, bromate formation increased drastically to concentrations of up to 103 µg L^{-1}, resulting in a molar bromide to bromate conversion of up to 78 %. A similar relationship between bromate formation and ozone dose has been described previously for wastewater effluents and surface water (Li et al., 2017), indicating that these results can also be translated into groundwater treatment. At specific ozone doses below 0.5 mg O_3/mg DOC, single-tube ozonation resulted in lower or similar bromate formation compared to batch ozonation. This was inverted at higher ozone doses, which resulted in significantly higher bromate concentrations of single-tube compared to batch ozonation. Similarly, it was found in previous studies that bromate formation in membrane peroxone processes may either be lower or higher than in batch peroxone processes (Merle et al., 2017; Stylianou et al., 2018b). Lower bromate formation in the membrane peroxone process than in batch ozonation was only found at ozone gas concentrations of 0.5–1.0 g O_3 m^{-3} (Merle et al., 2017), which is more than one order of magnitude lower than used in the study presented here. In single-tube ozonation, a decrease in bromate concentration was observed with increasing hydraulic retention time, i.e. with decreasing ozone gas concentration, at comparable ozone dose (Fig. 5.b, clusters I and II). This is in agreement with the results of previous studies on membrane peroxone application (Merle et al., 2017; Stylianou et al., 2018b) and suggests that bromate control in NOM-rich groundwater may be achieved without addition of H_2O_2. Multi-tube membrane ozonation produced higher bromate concentrations than the other two setups tested despite longer hydraulic retention times and lower ozone gas concentrations than used in the single-tube contactor. The higher bromate formation in the multi-tube contactor may be due to the uneven ozone distribution within the module. We assume that bromate formation was higher in some membrane fibers due to elevated ozone dose, which might have resulted in an increased bromate concentration of the final contactor effluent. In the multi-tube contactor, only slight variation in bromate formation was observed, which may be due to the small variation in experimental conditions (see above).

Figure S9 shows color (VIS_{436}) versus bromate for all ozonation setups. At comparable VIS_{436} abatement, bromate formation was in the order batch ≈ single-tube contactor < multi-tube contactor, indicating more selective VIS_{436} reduction over bromate formation in batch and single-tube ozonation. At enhanced color removal, i.e., $VIS_{436} < 0.3$ m^{-1}, bromate formation in the single-tube contactor was higher than in batch ozonation. These results are in accordance with the varying bromate formation in the different ozonation setups (Fig. 5.b). At bromate concentrations below 10 µg L^{-1}, color removal of up to 45 % for the single-tube contactor and batch ozonation and 17 % for the multi-tube contactor could be achieved. The color removal performance by ozonation in other groundwaters may be higher as the increase in color at low ozone doses shown here was not observed in the ozonation of other groundwaters (Rittmann et al., 2002; Sobhani et al., 2012).

Fig. 5.c shows Ha for membrane ozonation as a function of specific ozone dose. Ha decreased with specific ozone dose because of decreasing ozone decay rate k_{O3}. At constant specific ozone dose, Ha increased with increasing hydraulic retention time and therefore decreasing flow velocity (Zoumpouli et al., 2018). Clusters I and II of Fig. 5.c highlight data points with comparable ozone dose and increase of Ha with hydraulic retention time. For these clusters, bromate formation decreased for increasing hydraulic retention time and therefore higher Ha, as highlighted in Fig. 5.b. Ha indicates if the ozone concentration in the liquid film is controlled by mass transfer or reaction. At increased Ha, mass transfer limitation and therefore competition between different reactants for ozone may increase (Beltrán, 1995). It is plausible that high

reaction rates of NOM with ozone may decrease ozone exposure for compounds with slower ozone reaction kinetics and thereby decrease bromate formation at increased Ha.

Despite higher Ha in the multi-tube contactor than in the single-tube contactor, at comparable ozone dose (Fig. 5.c), bromate formation was higher in the multi-tube contactor (Fig. 5.b). Ha was calculated for the overall ozone dose charged to the multi-tube contactor. As the ozone dose is assumed to vary within the membrane fibers (see above), Ha is also expected to vary. This makes direct comparison to a single-tube contactor less straightforward.

Ha > 1, i.e., faster reaction than mass transfer rate in the liquid film (Leiknes et al., 2005) were obtained at specific ozone doses < 0.5 mg O_3/mg DOC for both membrane contactors. At these ozone doses, bromate formation was similar in the single-tube contactor compared to batch ozonation (Fig. 5b). At higher ozone dose, bromate formation in the single-tube contactor exceeded bromate formation in batch ozonation. The application of ozone doses > 0.5 mg O_3/mg DOC at a lower bromate formation than observed here might be feasible if the ozone gas concentration is further decreased and the hydraulic retention time is further increased.

The use of Ha to indicate enhanced competition between NOM degradation and bromate formation in membrane ozonation may help in experimental and contactor design to perform membrane ozonation under mass-transfer limited conditions. This knowledge may be applied to other treatment targets that aspire selective ozonation. Zero-outlet ozone concentrations can serve as an indicator for high Ha (Fig. 3).

Membrane contactor design to achieve high Ha would imply both large diameter and length, as both decrease k_L (Eq. (2), eq. S1–S4). As k_L is usually the limiting factor for mass transfer in membrane ozonation (Pines et al., 2005), this may increase the capital costs and footprint of membrane ozonation contactors. On the other hand, the pumping energy demand may be reduced at low flow velocities (Gottschalk et al., 2010). Large-scale energy demand and cost assessments of membrane ozonation are required to fully assess the potential of membrane ozonation under different operating conditions (Bein et al., 2020). To induce more uniform mass transfer conditions in multi-tube hollow fiber modules, ozone gas distribution should be optimized, e.g. by increasing the distance between the tubes.

4. Conclusions

- Color (VIS_{436}) and ultraviolet light absorbance (UV_{254}) of a groundwater could be significantly reduced by ozonation. However, high bromide levels resulted in bromate concentrations beyond the WHO guideline value (10 µg L^{-1}) for specific ozone doses > 0.5 mg O_3/mg DOC. At lower ozone doses, high reaction rates of natural organic matter (NOM) and ozone resulted in low dissolved ozone concentrations and controlled bromate formation.
- In membrane ozonation, conditions associated with a low mass transfer rate (low ozone gas concentration, long hydraulic retention time, high Hatta number (Ha)) showed lower bromate formation at comparable ozone dose than inverse conditions.
- Bromate formation in the single-tube contactor was higher than in batch ozonation if specific ozone doses > 0.5 mg O_3/mg DOC were applied with Ha < 1. At specific ozone doses < 0.5 mg O_3/mg DOC, bromate formation was comparable or lower in single-tube ozonation compared to batch ozonation. This was associated with Ha > 1, which implies mass transfer limitation of ozone in the membrane contactor. Longer hydraulic retention time and lower ozone gas concentrations may further depress bromate formation also at higher ozone doses.
- As process settings with high Ha were beneficial for increasing the selectivity of NOM degradation over bromate formation, further research is needed on large-scale implementation of high Ha membrane ozonation design for optimization of both water quality and treatment costs.
- Dissolved ozone concentration at the membrane ozonation contactor outlet might be a useful and simple parameter to assess Ha of the process. Zero-outlet concentrations of dissolved ozone were measured for Ha > 1 in single-tube ozonation and Ha > 1.67 in multi-tube ozonation.
- Uneven transversal ozone distribution inside a multi-tube contactor appeared to increase bromate formation, which was generally higher compared to single-tube ozonation at comparable ozone dose and Ha. Thus, specific ozone dose and Ha are not recommended as the only parameters to explain differences in water quality after treatment by different membrane contactors. The identification of further parameters to quantify ozonation selectivity of target compound removal over by-product formation in membrane contactors warrants further research.

Declaration of Competing Interest

The authors declare that they have no known competing financial interests or personal relationships that could have appeared to influence the work reported in this paper.

Acknowledgements

The authors would like to thank the German Technical and Scientific Association for Gas and Water (DVGW) and associated water suppliers for funding the project “COL_EX” (W 201719). Garyfalia A. Zoumpouli was supported by a University of Bath research scholarship and a UK Engineering and Physical Research Council (EPSRC) funded Integrated PhD studentship in Sustainable Chemical Technologies: EP/L016354/1. Also, the authors would like to thank Lutz Imhof (TZW Dresden) for the LC-OCD analyses that were made for this study.

Supplementary materials

Supplementary material associated with this article can be found, in the online version, at doi:10.1016/j.watres.2022.118739.

References

Alhweij, H., Emanuelsson, E.A.C., Shahid, S., Wenk, J., 2022. Organic matter removal and antifouling performance of sulfonated polyaniline nanofiltration (S-PANI NF) membranes. J. Environ. Chem. Eng. 10 (3), 107906 https://doi.org/10.1016/j.jece.2022.107906.

Atchariyawut, S., Jiraratananon, R., Wang, R., 2007. Separation of CO2 from CH4 by using gas–liquid membrane contacting process. J. Membr. Sci. 304 (1-2), 163–172.

Bader, H., Hoigné, J., 1981. Determination of ozone in water by the indigo method. Water Res. 15 (4), 449–456.

Bein, E., Zucker, I., Drewes, J.E., Hübner, U., 2020. Ozone membrane contactors for water and wastewater treatment: a critical review on materials selection, mass transfer and process design. Chem. Eng. J., 127393

Beltrán, F.J., 1995. Theoretical aspects of the kinetics of competitive ozone reactions in water. Ozone Sci. Eng. 17 (2), 163–181.

Beniwal, D., Taylor-Edmonds, L., Armour, J., Andrews, R.C., 2018. Ozone/peroxide advanced oxidation in combination with biofiltration for taste and odour control and organics removal. Chemosphere 212, 272–281.

Berry, M., Taylor, C., King, W., Chew, Y., Wenk, J., 2017. Modelling of ozone mass-transfer through non-porous membranes for water treatment. Water 9 (7), 452.

Brezonik, P., Arnold, W., 2011. Water Chemistry: Water Chemistry An Introduction to the Chemistry of Natural and Engineered Aquatic Systems. Oxford University Press, Oxford, UK.

Buffle, M.-O., Schumacher, J., Meylan, S., Jekel, M., von Gunten, U., 2006. Ozonation and advanced oxidation of wastewater: effect of O3 dose, pH, DOM and HO• -scavengers on ozone decomposition and HO• generation. Ozone Sci. Eng. 28 (4), 247–259.

Charpentier, J.-C., 1981. Mass-transfer rates in gas-liquid-absorbers and reactors. Eds.. In: Drew, T.B., Cokelet, G.R., Hoopes Jr, J.W., Vermeulen, T. (Eds.), Advances in Chemical Engineering, 11 ed. Advances in Chemical Engineering. Academic Press, New York, 11.1981.

Chon, K., Salhi, E., von Gunten, U., 2015. Combination of UV absorbance and electron donating capacity to assess degradation of micropollutants and formation of bromate during ozonation of wastewater effluents. Water Res. 81, 388–397.

Crittenden, J.C., Trussell, R.R., Hand, David, W., Howe, K.J., Tchobanoglous, G., 2012. MWH's Water Treatment: Principles and Design, 3rd ed. John Wiley & Sons, Inc., Hoboken, New Jersey, USA.

Drinkwaterbesluit, 2011. Besluit van 23 mei 2011, houdende bepalingen inzake de productie en distributie van drinkwater en de organisatie van de openbare drinkwatervoorziening (Drinkwaterbesluit).
Elovitz, M.S., von Gunten, U., Kaiser, H.-P., 2000. Hydroxyl Radical/Ozone ratios during ozonation processes. II. The effect of temperature, pH, Alkalinity, and DOM properties. Ozone Sci. Eng. 22 (2), 123–150.
EU, 1998. Council Directive 98/83/EC of 3 November 1998 on the quality of water intended for human consumption.
Frimmel, F.H., 1998. Characterization of natural organic matter as major constituents in aquatic systems. J. Contam. Hydrol. 35 (1), 201–216.
Gerrity, D., Snyder, S., 2011. Review of ozone for water reuse applications: toxicity, regulations, and trace organic contaminant oxidation. Ozone Sci. Eng. 33 (4), 253–266.
Gottschalk, C., Libra, J.A., Saupe, A., 2010. Ozonation of Water and Waste Water: A Practical Guide to Understanding Ozone and Its Applications, 2., Completely Rev. Wiley-VCH, Weinheim updated ed. ed.
Heeb, M.B., Criquet, J., Zimmermann-Steffens, S.G., von Gunten, U., 2014. Oxidative treatment of bromide-containing waters: formation of bromine and its reactions with inorganic and organic compounds–a critical review. Water Res. 48, 15–42.
Hooper, J., Funk, D., Bell, K., Noibi, M., Vickstrom, K., Schulz, C., Machek, E., Huang, C.-H., 2020. Pilot testing of direct and indirect potable water reuse using multi-stage ozone-biofiltration without reverse osmosis. Water Res. 169, 115178.
Hübner, U., Miehe, U., Jekel, M., 2012. Optimized removal of dissolved organic carbon and trace organic contaminants during combined ozonation and artificial groundwater recharge. Water Res. 46 (18), 6059–6068.
ISO, 2011. Water quality - Determination of dissolved bromate - Method using ion chromatography (IC) and post column reaction (PCR) (ISO 11206:2011). Beuth Verlag GmbH, Berlin, 13.060.50. doi:10.31030/1972886.
Jansen, R., Rijk, J.W.de, Zwijnenburg, A., Mulder, M., Wessling, M., 2005. Hollow fiber membrane contactors—A means to study the reaction kinetics of humic substance ozonation. J. Membr. Sci. 257 (1-2), 48–59.
Kaprara, E., Kostoglou, M., Koutsiantzi, C., Psaltou, S., Zouboulis, A.I., Mitrakas, M., 2020. Enhancement of ozonation efficiency employing dead-end hollow fiber membranes. Environ. Sci. 6 (9), 2619–2627.
Kwon, M., Kye, H., Jung, Y., Yoon, Y., Kang, J.-W., 2017. Performance characterization and kinetic modeling of ozonation using a new method: ROH,O3 concept. Water Res. 122, 172–182.
Leenheer, J.A., Croué, J.-P., 2003. Characterizing aquatic dissolved organic matter. Environ. Sci. Technol. 37 (1), 18A–26A.
Leiknes, T., Phattaranawik, J., Boller, M., von Gunten, U., Pronk, W., 2005. Ozone transfer and design concepts for NOM decolourization in tubular membrane contactor. Chem. Eng. J. 111 (1), 53–61.
Leresche, F., McKay, G., Kurtz, T., von Gunten, U., Canonica, S., Rosario-Ortiz, F.L., 2019. Effects of ozone on the photochemical and photophysical properties of dissolved organic matter. Environ. Sci. Technol. 53 (10), 5622–5632.
Lévêque, A., 1928. The laws of heat transfer by convection (Original language: Les Lois de la transmission de chaleur par convection). Dunod.
Li, W.-T., Cao, M.-J., Young, T., Ruffino, B., Dodd, M., Li, A.-M., Korshin, G., 2017. Application of UV absorbance and fluorescence indicators to assess the formation of biodegradable dissolved organic carbon and bromate during ozonation. Water Res. 111, 154–162.
Tan, Lo, Johnson, W., 2001. Removing organic color and by-products from groundwater with ozone and pressurized biologically-active filtration. Ozone Sci. Eng. 23 (5), 393–400.
McDonough, L.K., Santos, I.R., Andersen, M.S., O'Carroll, D.M., Rutlidge, H., Meredith, K., Oudone, P., Bridgeman, J., Gooddy, D.C., Sorensen, J.P.R., Lapworth, D.J., MacDonald, A.M., Ward, J., Baker, A., 2020. Changes in global groundwater organic carbon driven by climate change and urbanization. Nat. Commun. 11 (1), 1279.
Merle, T., Pronk, W., von Gunten, U., 2017. MEMBRO 3 X, a novel combination of a membrane contactor with advanced oxidation (O 3 /H 2 O 2) for simultaneous micropollutant abatement and bromate minimization. Environ. Sci. Technol. Lett. 4 (5), 180–185.
Nöthe, T., Fahlenkamp, H., Sonntag, C.v., 2009. Ozonation of wastewater: rate of ozone consumption and hydroxyl radical yield. Environ. Sci. Technol. 43 (15), 5990–5995.
Önnby, L., Salhi, E., McKay, G., Rosario-Ortiz, F.L., von Gunten, U., 2018. Ozone and chlorine reactions with dissolved organic matter - Assessment of oxidant-reactive moieties by optical measurements and the electron donating capacities. Water Res. 144, 64–75.
Phattaranawik, J., Leiknes, T., Pronk, W., 2005. Mass transfer studies in flat-sheet membrane contactor with ozonation. J. Membr. Sci. 247 (1-2), 153–167.
Pines, D.S., Min, K.-N., Ergas, S.J., Reckhow, D.A., 2005. Investigation of an ozone membrane contactor system. Ozone Sci. Eng. 27 (3), 209–217.
Pinkernell, U., von Gunten, U., 2001. Bromate minimization during ozonation: mechanistic considerations. Environ. Sci. Technol. 35 (12), 2525–2531.
Pocostales, J.P., Sein, M.M., Knolle, W., Sonntag, C.v., Schmidt, T.C., 2010. Degradation of ozone-refractory organic phosphates in wastewater by ozone and ozone/hydrogen peroxide (peroxone): the role of ozone consumption by dissolved organic matter. Environ. Sci. Technol. 44 (21), 8248–8253.
Regan, S., Hynds, P., Flynn, R., 2017. An overview of dissolved organic carbon in groundwater and implications for drinking water safety. Hydrol. J. 25 (4), 959–967.
Remucal, C.K., Salhi, E., Walpen, N., von Gunten, U., 2020. Molecular-level transformation of dissolved organic matter during oxidation by ozone and hydroxyl radical. Environ. Sci. Technol. 54 (16), 10351–10360.
Rittmann, B.E., Stilwell, D., Garside, J.C., Amy, G.L., Spangenberg, C., Kalinsky, A., Akiyoshi, E., 2002. Treatment of a colored groundwater by ozone-biofiltration: pilot studies and modeling interpretation. Water Res. 36 (13), 3387–3397.
Rougé, V., von Gunten, U., Allard, S., 2020. Efficiency of pre-oxidation of natural organic matter for the mitigation of disinfection byproducts: electron donating capacity and UV absorbance as surrogate parameters. Water Res. 187, 116418.
Rutlidge, H., McDonough, L.K., Oudone, P., Andersen, M.S., Meredith, K., Chinu, K., Peterson, M., Baker, A., 2021. Characterisation of groundwater dissolved organic matter using LC-OCD: implications for water treatment. Water Res. 188, 116422.
Schmitt, A., Mendret, J., Roustan, M., Brosillon, S., 2020. Ozonation using hollow fiber contactor technology and its perspectives for micropollutants removal in water: a review. Sci. Total Environ. 729, 138664.
Schulz, M., 2020. Removal of Natural Organic Matter by Coagulation-UF during Treatment of Anoxic Groundwaters (Original language: Entfernung natürlicher organischer Stoffe durch die Verfahrenskombination Flockung-Ultrafiltration bei der Aufbereitung reduzierter Grundwässer). Doctoral Thesis. Hamburg University of Technology.
Sharpless, C.M., Blough, N.V., 2014. The importance of charge-transfer interactions in determining chromophoric dissolved organic matter (CDOM) optical and photochemical properties. Environ. Sci. 16 (4), 654–671.
Sillanpää, M., 2015. Natural Organic Matter in Water: Characterization and Treatment Methods. Butterworth-Heinemann, Oxford, England.
Sobhani, R., McVicker, R., Spangenberg, C., Rosso, D., 2012. Process analysis and economics of drinking water production from coastal aquifers containing chromophoric dissolved organic matter and bromide using nanofiltration and ozonation. J. Environ. Manage. 93 (1), 209–217.
Soltermann, F., Abegglen, C., Tschui, M., Stahel, S., von Gunten, U., 2017. Options and limitations for bromate control during ozonation of wastewater. Water Res. 116, 76–85.
Song, R., Donohoe, C., Minear, R., Westerhoff, P., Ozekin, K., Amy, G., 1996. Empirical modeling of bromate formation during ozonation of bromide-containing waters. Water Res. 30 (5), 1161–1168.
Stylianou, S.K., Katsoyiannis, I.A., Ernst, M., Zouboulis, A.I., 2018a. Impact of O3 or O3/H2O2 treatment via a membrane contacting system on the composition and characteristics of the natural organic matter of surface waters. Environ. Sci. Pollut. Res. 25 (13), 12246–12255.
Stylianou, S.K., Katsoyiannis, I.A., Mitrakas, M., Zouboulis, A.I., 2018b. Application of a ceramic membrane contacting process for ozone and peroxone treatment of micropollutant contaminated surface water. J. Hazard. Mater. 358, 129–135.
Stylianou, S.K., Kostoglou, M., Zouboulis, A.I., 2016. Ozone mass transfer studies in a hydrophobized ceramic membrane contactor: experiments and analysis. Ind. Eng. Chem. Res. 55 (28), 7587–7597.
Trinkwasserverordnung, 2001. Trinkwasserverordnung in der Fassung der Bekanntmachung vom 10. März 2016 (BGBl. I S. 459), die zuletzt durch Artikel 1 der Verordnung vom 22. September 2021 (BGBl. I S. 4343) geändert worden ist: TrinkwV.
Tubić, A., Agbaba, J., Dalmacija, B., Perović, S.U., Klašnja, M., Rončević, S., Ivančev-Tumbas, I., 2011. Removal of natural organic matter from groundwater using advanced oxidation processes at a pilot scale drinking water treatment plant in the Central Banat Region (Serbia). Ozone Sci. Eng. 33 (4), 267–278.
Twardowski, M.S., Boss, E., Sullivan, J.M., Donaghay, P.L., 2004. Modeling the spectral shape of absorption by chromophoric dissolved organic matter. Mar. Chem. 89 (1-4), 69–88.
Tyrovola, K., Diamadopoulos, E., 2005. Bromate formation during ozonation of groundwater in coastal areas in Greece. Desalination 176 (1), 201–209.
USEPA, 2009. National Primary Drinking Water Regulations.
von Gunten, U., 2003. Ozonation of drinking water: Part II. Disinfection and by-product formation in presence of bromide, iodide or chlorine. Water Res. 37 (7), 1469–1487.
von Gunten, U., 2018. Oxidation processes in water treatment: are we on track? Environ. Sci. Technol. 52 (9), 5062–5075.
von Sonntag, C., von Gunten, U., 2012. Chemistry of Ozone in Water and Wastewater Treatment: From Basic Principles to Applications. IWA Publishing, London.
Walpen, N., Houska, J., Salhi, E., Sander, M., von Gunten, U., 2020. Quantification of the electron donating capacity and UV absorbance of dissolved organic matter during ozonation of secondary wastewater effluent by an assay and an automated analyzer. Water Res. 185, 116235.
Wenk, J., Aeschbacher, M., Salhi, E., Canonica, S., von Gunten, U., Sander, M., 2013. Chemical oxidation of dissolved organic matter by chlorine dioxide, chlorine, and ozone: effects on its optical and antioxidant properties. Environ. Sci. Technol. 47 (19), 11147–11156.
Wert, E.C., Rosario-Ortiz, F.L., Snyder, S.A., 2009. Using ultraviolet absorbance and color to assess pharmaceutical oxidation during ozonation of wastewater. Environ. Sci. Technol. 43 (13), 4858–4863.
Westerhoff, P., Aiken, G., Amy, G., Debroux, J., 1999. Relationships between the structure of natural organic matter and its reactivity towards molecular ozone and hydroxyl radicals. Water Res. 33 (10), 2265–2276.
Westerhoff, P., Song, R., Amy, G., Minear, R., 1998. NOM's role in bromine and bromate formation during ozonation. J. Am. Water Works Assoc. 90 (2), 82–94.
WHO, 2017. Guidelines for Drinking-Water Quality, Fourth Edition Incorporating the First Addendum Ed. World Health Organization, Geneva.
Yang, J., Dong, Z., Jiang, C., Wang, C., Liu, H., 2019. An overview of bromate formation in chemical oxidation processes: Occurrence, mechanism, influencing factors, risk assessment, and control strategies. Chemosphere 237, 124521.

Ying, Z., Yecheskel, Y., Huo, M., Hübner, U., Zucker, I., 2021. Ozone Consumption by soils: a critical factor in in situ ozonation processes. ACS ES&T Water 1 (11), 2403–2411.
Zoumpouli, G.A., Baker, R., Taylor, C.M., Chippendale, M.J., Smithers, C., Xian, S.H., Mattia, D., Chew, Y.M.J., Wenk, J., 2018. A single tube contactor for testing membrane ozonation. Water (1416), 10.
Zucker, I., Mamane, H., Cikurel, H., Jekel, M., Hübner, U., Avisar, D., 2015. A hybrid process of biofiltration of secondary effluent followed by ozonation and short soil aquifer treatment for water reuse. Water Res. 84, 315–322.